Transformed Fourier and Fick equations for the control of heat and mass diffusion

Sebastien Guenneau, D Petiteau, Myriam Zerrad, Claude Amra, Tania Puvirajesinghe

AIP | Advances

Transformed Fourier and Fick equations for the control of heat and mass diffusion

S. Guenneau, D. Petiteau, M. Zerrad, C. Amra, and T. Puvirajesinghe

Citation: AIP Advances **5**, 053404 (2015); doi: 10.1063/1.4917492
View online: http://dx.doi.org/10.1063/1.4917492
View Table of Contents: http://scitation.aip.org/content/aip/journal/adva/5/5?ver=pdfcov
Published by the AIP Publishing

Transformed Fourier and Fick equations for the control of heat and mass diffusion

S. Guenneau,[1] D. Petiteau,[1] M. Zerrad,[1] C. Amra,[1] and T. Puvirajesinghe[2]
[1]*Aix–Marseille Université, UMR CNRS 7249, Centrale Marseille, Institut Fresnel, 13013 Marseille, France*
[2]*Aix–Marseille Université, UMR CNRS 7258, UMR INSERM 1068, Centre de Recherche en Cancérologie de Marseille, Institut Paoli-Calmettes, 13009 Marseille, France*

(Received 12 February 2015; accepted 31 March 2015; published online 9 April 2015)

We review recent advances in the control of diffusion processes in thermodynamics and life sciences through geometric transforms in the Fourier and Fick equations, which govern heat and mass diffusion, respectively. We propose to further encompass transport properties in the transformed equations, whereby the temperature is governed by a three-dimensional, time-dependent, anisotropic heterogeneous convection-diffusion equation, which is a parabolic partial differential equation combining the diffusion equation and the advection equation. We perform two dimensional finite element computations for cloaks, concentrators and rotators of a complex shape in the transient regime. We precise that in contrast to invisibility cloaks for waves, the temperature (or mass concentration) inside a diffusion cloak crucially depends upon time, its distance from the source, and the diffusivity of the invisibility region. However, heat (or mass) diffusion outside cloaks, concentrators and rotators is unaffected by their presence, whatever their shape or position. Finally, we propose simplified designs of layered cylindrical and spherical diffusion cloaks that might foster experimental efforts in thermal and biochemical metamaterials. [http://dx.doi.org/10.1063/1.4917492]

I. INTRODUCTION

There is currently a keen interest in the control of heat flux using thermal metamaterials in steady,[1–7] transient[8–12] and periodic[13] regimes. In the present paper, we discuss the functionality of diffusion cloaks for heat and mass, as well as concentrators and rotators,[14] via transformed Fourier[8,15] and Fick[16–18] equations.

Such designs are based upon the extension of metamaterials designed using tools of transformation optics to the fields of thermodynamics and biochemistry. Let us note that cloaking for diffusion processes[19,20] is more subtle than for waves[21–28] wherein the field vanishes in the invisibility region irrespective of its material constituent, time and its distance of the source. This appears to be in sharp contrast with thermal cloaks wherein temperature inside the invisibility region (or mass concentration in the context of diffusion of chemical species) appears to depend on its diffusivity, upon time, and the distance from the source.

More precisely, in a way similar to the English physicist Pendry and his American colleagues Schurig and Smith who proposed in 2006 to design an invisibility cloak by mapping Maxwell's equations on a curvilinear space with a hole in it (where an object can be hidden), one can make coordinate changes in governing equations of thermodynamics and biochemistry[8,16] with convection diffusion phenomena.

The plan of the paper is as follows: In section II, we apply a change of coordinates to the diffusion-convection equation and show that the diffusivity becomes in general heterogeneous (i.e. spatially varying) and anisotropic (i.e. matrix valued). In section III, we apply specific mappings in order to make a hole in the transformed coordinates so as to design a cloak (with a

FIG. 1. Artistic representation of the potential use of a thermal cylindrical cloak for protection of a component on a computer motherboard.

blow-up of a point), a concentrator (with a compression of a region) and a rotator (with a rotation of axes) for heat flux or for mass concentration flux. We use finite element computations to validate our hypothesis of control of heat or concentration flux in the transformed thermal or chemical spaces. We also notably analyze the potential protection offered by diffusion cloaks, which could have potential applications in microelectronics, see Fig. 1 for an artistic view. In section IV, we propose a multilayered spherical device which approximates the functionality of a diffusion cloak in the homogenization regime.[13,29] In section V, we look at so-called diffusion carpet cloaks and we conclude the paper in section VI.

II. TRANSFORMED CONVECTION-DIFFUSION EQUATION

Let us consider the convection-diffusion equation which is a parabolic partial differential equation combining the diffusion equation and the advection equation. This equation describes physical phenomena where particles or energy (or other physical quantities) are transferred inside a physical system due to two processes: diffusion and convection. Let us assume that the diffusion coefficient and the convection velocity are constant and there are no sources or sinks in a bounded domain Ω (the source lies outside Ω). The convection-diffusion equation is then expressed as

$$\rho(\mathbf{x})c(\mathbf{x})\frac{\partial u}{\partial t} = \nabla \cdot (\kappa(\mathbf{x})\nabla u - \mathbf{v}(\mathbf{x})u) + p(\mathbf{x},t)\ , \tag{1}$$

where u denotes the distribution of temperature in thermodynamics (or mass concentration in biochemistry) at each point $\mathbf{x} = (x, y, z)$ within the domain Ω. In the transient regime, u also changes with time $t > 0$ (this is markedly different from the thermostatic case, where the left-hand side of (1) vanishes). We note that the coefficient κ is the thermal conductivity ($W.m^{-1}.K^{-1}$ i.e. watt per meter kelvin in SI units), ρ is the density ($kg.m^{-3}$ i.e. kilogram per cubic meter in SI units) and c the specific heat (or thermal) capacity ($J.K^{-1}.kg^{-1}$ i.e. joule per kilogram kelvin in SI units). The bulk velocity $\mathbf{v}$ has the unit of length by time. Similar coefficients hold in the mass diffusion case and they generally depend depend upon space and time variables. The diffusion flux $-\kappa\nabla u$ measures the amount of substance that will flow through a small volume during a small time interval ($mol.m^{-3}.s^{-1}$).

One can see at this point that if the medium has an anisotropic conductivity κ, heat will diffuse in awkward directions. Moreover, if the medium is heterogeneous (e.g. when κ is piecewise constant) the spatial derivatives of κ might suffer some jump, hence one could observe strong heat gradient at interfaces. In fact, transmission conditions ensuring continuity of heat u and heat flux $\kappa\nabla u$ are encompassed in Eq. (1) since derivatives are taken in distributional sense. Let us finally stress that in Eq. (1) the source term will be for our numerical purpose a time step (Heaviside) variation and a singular (Dirac) spatial variation, that is: $p(\mathbf{x},t) = p_0 H(t)\delta(\mathbf{x}-\mathbf{x}0)$, with H the Heaviside function and Delta the Dirac distribution. Physically speaking, the source term is constant throughout time $t > 0$ and it is spatially localized on the line $\mathbf{x} = \mathbf{x}_0$.

Let us now make the change of variable $(x, y, z) \rightarrow (x', y', z')$ in Eq. (1). We find that the transformed convection-diffusion equation has the form:

$$\begin{aligned}\rho(\mathbf{x}')c(\mathbf{x}')\det(\mathbf{J})\frac{\partial u}{\partial t} &= \nabla\cdot\left(\mathbf{J}^{-T}\kappa(\mathbf{x}')\mathbf{J}^{-1}\det(\mathbf{J})\nabla u\right.\\ &\left.-\mathbf{J}^{-T}\det(\mathbf{J})\mathbf{v}(\mathbf{x}')u\right) + \det(\mathbf{J})p(\mathbf{x}',t)\ ,\end{aligned} \tag{2}$$

where $\mathbf{J} = \partial(x', y', z')/\partial(x, y, z)$ is the Jacobian matrix. One can see that Eq. (1) and (2) share the same structure. This is better seen if we introduce the transformed diffusivity and velocity as

$$\underline{\underline{\kappa}}' = \mathbf{J}^{-T}\kappa\mathbf{J}^{-1}\det(\mathbf{J}) = \kappa\mathbf{J}^{-T}\mathbf{J}^{-1}\det(\mathbf{J}) = \kappa\mathbf{T}^{-1}\ ,\ \text{and}\ \mathbf{v}' = \mathbf{J}^{-T}\det(\mathbf{J})\mathbf{v}\ . \tag{3}$$

Clearly, $\underline{\underline{\kappa}}'$ is a matrix-valued field, whereas $\mathbf{v}'$ is a (heterogeneous) vector field. It is interesting to note that $\underline{\underline{\mathbf{T}}}$ is the metric tensor.

There are few ways to derive Eq. (2), but a simple one is to multiply (1) by a test function ϕ which is smooth with a compact support on Ω (i.e. it vanishes on the boundary of Ω). One can then integrate the resulting equation over Ω. After integration by parts, we are led to a weak form of Eq. (1):

$$\begin{aligned}&\int_\Omega \rho c\left(\frac{\partial u}{\partial t}\phi\right)dxdydz + \int_\Omega (\kappa\nabla u\cdot\nabla\phi)\,dxdydz\\ &-\int_\Omega \mathbf{v}u\cdot\nabla\phi dxdydz + < p,\phi >= 0\ ,\end{aligned} \tag{4}$$

where $<,>$ denotes the duality product between the space of distributions and the space of smooth functions (in which one integrates a distribution multiplied by a test function), see Ref. 29.

It is easy to make the coordinate change $(x, y, z) \rightarrow (x', y', z')$ in (4). For this, one notes that $\nabla = \mathbf{J}^{-1}\nabla'$, where ∇' is the gradient in the new coordinates and also one should keep in mind there is a change in the infinitesimal volume $dxdydz$ proportional to $det(\mathbf{J})$:

$$\begin{aligned}&\int_\Omega\left(\rho c\det(\mathbf{J})\frac{\partial u}{\partial t}\phi\right)dx'dy'dz' + \int_\Omega\left\{\left(\mathbf{J}^{-1}\nabla'\phi\cdot\kappa\mathbf{J}^{-1}\nabla' u\right)\det(\mathbf{J})\right\}dx'dy'dz'\\ &-\int_\Omega\left\{\left(\mathbf{J}^{-1}\nabla'\phi\cdot\mathbf{v}\nabla' u\right)\det(\mathbf{J})\right\}dx'dy'dz' + < \det(\mathbf{J})p,\phi >= 0\ .\end{aligned} \tag{5}$$

Equation (5) is the weak form of (2). In order to see this, one should integrate by parts, and note that $\mathbf{J}^{-1}\nabla'\phi\cdot\kappa\mathbf{J}^{-1}\nabla' u = (\nabla'\phi)^T\mathbf{J}^{-T}\kappa\mathbf{J}^{-1}\nabla' u$. We further note that Fick's equation which is used in the context of mass diffusion is encompassed by the convection-diffusion equation (take the product ρc to be equal to 1 and assume that the velocity field $\mathbf{v}$ vanishes. Thus, what we discuss in the sequel applies straightforwardly to mass diffusion.

III. DIFFUSION INVISIBILITY CLOAK, CONCENTRATOR AND ROTATOR OF AN ARBITRARY SHAPE

We now wish to implement the transformed diffusion-convection Eq. (2) in order to design three heterogeneous anisotropic media with specific functionalities: an invisibility cloak, a concentrator and a rotator for heat flux (or mass diffusion). In order to describe boundaries of general

shapes, a finite Fourier expansion

$$\rho(\theta) = a_0 + \sum_{k=1}^{n} (a_k \cos(k\theta) + b_k \sin(k\theta)) \,, \tag{6}$$

may be used. Throughout this section, we consider a linear transform:

$$\rho'(\rho, \theta) = \alpha\rho + \beta \tag{7}$$

where α and β are θ dependent coefficients, with $0 < \theta \leq 2\pi$. In this way, we can design some cloak, concentrator and rotator of a complex shape. For the sake of illustration, we shall consider three boundaries with up to three terms in the Fourier expansion:

$$\begin{cases} R_1(\theta) = 0.4R(1 + 0.2\sin(3\theta)) \quad ; \quad R_2(\theta) = 0.6R(1 + 0.2\sin(3\theta)) \\ \qquad R = 0.4 \quad ; \quad R_3(\theta) = R(1 + 0.2(\sin(3\theta) + \cos(4\theta))) \end{cases} \tag{8}$$

A. Diffusion cloak

One can see in Figure 2 that heat flux (resp. mass in the context of biochemistry[16] or chemical engineering[17]) is smoothly detoured around the core of the cloak. Moreover, the cloak is itself transparent for heat since the isothermal lines are unperturbed outside this metamaterial. More precisely, we consider the geometric transform (7) with parameters

$$\alpha = \frac{R_3(\theta) - R_1(\theta)}{R_3(\theta)} \,, \; \beta = R_1(\theta) \,, \; R_1(\theta) \leq r \leq R_3(\theta) \,. \tag{9}$$

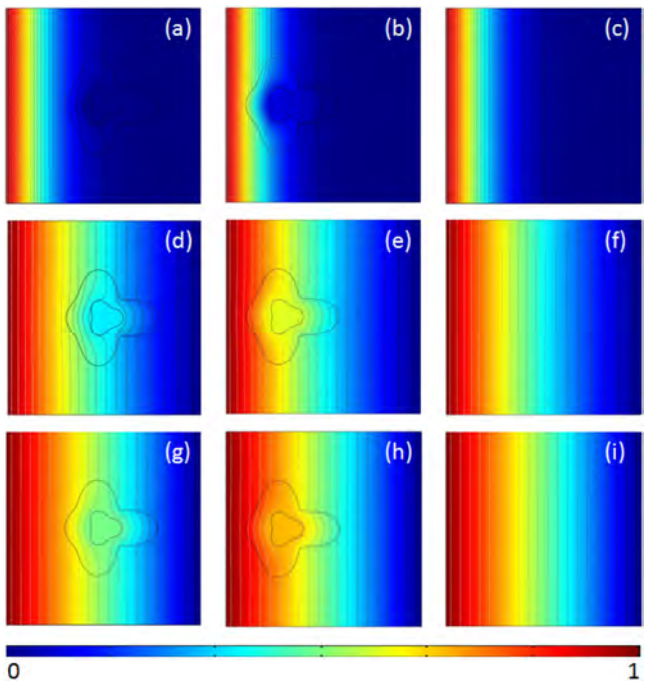

FIG. 2. Diffusion cloak: (Left panel) Diffusion of heat (or mass) from the left on a cloak of complex shape of inner radius $R_1(\theta) = 0.4R(1 + 0.2\sin(3\theta))$ and outer radius $R_3(\theta) = R(1 + 0.2(\sin(3\theta) + \cos(4\theta)))$, with $R = 0.4\ 10^{-4}$ m. The cloak is placed close to the source (left), further away (middle) and removed (right). Snapshots of heat distribution at $t = 0.001s$ (a,b,c), $t = 0.07s$ (d,e,f) and $t = 0.21s$ (g,h,i) show that isovalues of temperature (resp. mass) are nearly unperturbed outside the cloak. One notes the maximum temperature (resp. mass) in the core of the cloak is achieved for $t \geq 21s$ and depends upon the distance between the center of the cloak to the source.

We obtain the following Jacobian and transformation matrices ($\mathbf{R}(\theta)$ is the matrix of rotation through an angle θ):

$$\mathbf{J_{rr'}} = \begin{pmatrix} 1 & 0 \\ -\alpha & c_{22} \end{pmatrix} \quad \Longrightarrow \quad \mathbf{T^{-1}} = \mathbf{R}(\theta) \begin{pmatrix} \dfrac{(r-\beta)^2 + c_{22}^2.\alpha^2}{(r-\beta).r} & -\dfrac{c_{22}.\alpha}{r-\beta} \\ -\dfrac{c_{22}.\alpha}{r-\beta} & \dfrac{r}{r-\beta} \end{pmatrix} \mathbf{R}(\theta)^{\mathbf{T}} \tag{10}$$

with $\det(\mathbf{J}) = (r-\beta)/(\alpha^2 r)$ and

$$c_{22} = \frac{-1}{(R_2(\theta) - R_1(\theta))^2} \left\{ \frac{\partial R_1(\theta)}{\partial \theta} (R_3(\theta) - r)(R_3(\theta)) \right\} . \tag{11}$$

The numerical results performed with the finite element package COMSOL are shown in Figure 2. It is interesting to examine the thermal cloak parameter values at its non-reflecting outer boundary $R_2(\theta)$. This can be done through the analysis of the entries of the inverse of the metric tensor $\mathbf{T}$ in the polar basis. We first notice that the off-diagonal terms $(T^{-1})_{r\theta} = (T^{-1})_{\theta r}$ are generally nonzero unlike for the circular case when $\mathbf{T}^{-1}$ is diagonal. In general we observe that $-1 < (T^{-1})_{r\theta} < 1$, which reflects the rotation of the tensor $\mathbf{T}^{-1}$ with respect to its eigenbasis. We further note that $(T^{-1})_{rr}$ also varies with θ, unlike for circular thermal cloaks. Last, $0 < (T^{-1})_{rr} < 1$ and $(T^{-1})_{\theta\theta} > 1.5$, in agreement with the fact that the cloak ought to exhibit a strong azimuthal anisotropy for heat to flow around the inner core.

It is illuminating to compare these numerical results carried out in the intense near-field limit, to those obtained from an analytical approach, in order to better understand how this thermal cloak works. The temperature (resp. mass) field u is given in the transformed coordinates by

$$u'(\rho', \theta') := u(\rho(\rho', \theta'), \theta(\theta')) \tag{12}$$

with $\rho(\rho', \theta')$ and $\theta(\theta')$ given by the inverse map of the map defined by Eq. (9). We used the software Matlab to produce the map of isothermal values, see Fig. 3. Comparing this ideal thermal (resp. mass diffusion) cloaking with that of Fig. 2, we notice that the temperature (resp. mass) inside the invisibility region (inner core) of the cloak has the same value at any time step as the temperature (resp. mass) at the point that we blow up in the original coordinate system. This form of protection is markedly different from what is achieved with invisibility cloaks for waves. In the latter case, the field vanishes inside the invisibility region, whereas in the former case the field is uniform but not zero therein.

B. Diffusion concentrator

We now propose to extend the design of circular concentrators for heat[8] to more complex shapes. For the sake of simplicity, we consider a concentrator with the same boundaries as in (8). One can see in Figure 4 that heat (resp. mass concentration) isovalues are smoothly squeezed (hence the flux is enhanced) within the concentrator. Moreover, the concentrator is itself invisible for heat (resp. mass) as the isothermal lines are unperturbed outside this metamaterial. More precisely, we consider the geometric transform (7) with parameters:

$$\begin{cases} \alpha = \dfrac{R_1(\theta)}{R_2(\theta)} & \beta = 0 & (0 \le r \le R_1(\theta)) \\ \alpha = \dfrac{R_3(\theta) - R_1(\theta)}{R_3(\theta) - R_2(\theta)} & \beta = R_3(\theta)\dfrac{R_1(\theta) - R_2(\theta)}{R_3(\theta) - R_2(\theta)} & (R_1(\theta) \le r \le R_3(\theta)) \end{cases} \tag{13}$$

We obtain the same Jacobian and transformation matrices as in (10). However, the expression for entry c_{22} has changed:

• $0 \le r \le R_1(\theta)$:

$$c_{22} = \frac{\partial r}{\partial \theta'} = -\frac{r}{R_1(\theta)^2} \left(R_2(\theta) \frac{\partial R_1(\theta)}{\partial \theta} - R_1(\theta) \frac{\partial R_2(\theta)}{\partial \theta} \right) \tag{14}$$

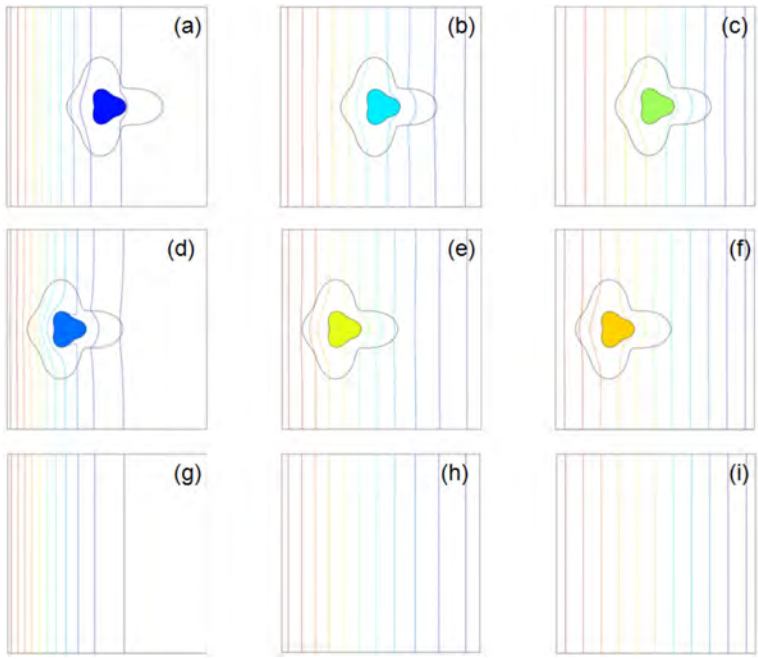

FIG. 3. Diffusion cloak: (Left panel) Diffusion of heat (or mass) from the left on a cloak of complex shape of inner radius $R_1(\theta) = 0.4R(1 + 0.2\sin(3\theta))$ and outer radius $R_3(\theta) = R(1 + 0.2(\sin(3\theta) + \cos(4\theta)))$, with $R = 0.4\ 10^{-4}$ m. The cloak is placed far from the source (top), closer (middle) and removed (bottom). Snapshots of heat (resp. mass) distribution at $t = 0.002s$ (a,d,g), $t = 0.07s$ (b,e,h) and $t = 0.21s$ (c,f,i) show that isovalues of temperature (resp. mass) are nearly unperturbed outside the cloak. One notes the maximum temperature (resp. mass) in the core of the cloak is achieved for $t \geq 21s$ and depends upon the distance between the center of the cloak to the source.

- $R_1(\theta) \leq r \leq R_3(\theta)$:

$$c_{22} = \frac{-1}{(R_2(\theta) - R_1(\theta))^2} \left\{ \frac{\partial R_1(\theta)}{\partial \theta}(R_3(\theta) - r)(R_3(\theta) - R_2(\theta)) + \frac{\partial R_2(\theta)}{\partial \theta}(R_1(\theta) - R_3(\theta))(R_3(\theta) - r) - \frac{\partial R_3(\theta)}{\partial \theta}(R_2(\theta) - R_1(\theta))(R_1(\theta) - r) \right\} . \quad (15)$$

C. Diffusion rotator

We now extend the design of circular cylindrical rotators for heat[15] to more complex geometries. For the sake of simplicity, we consider a rotator with the same boundaries as the cloak and concentrator, see (8). One can see in Figure 5 that heat (resp. mass) flux is smoothly rotated within the rotator (through an angle $\pi/4$). Moreover, the rotator is itself invisible for heat (resp. mass) as the isothermal values are unperturbed outside this metamaterial. It could be used to enhance thermal (or mass) exchanges.

In order to design the rotator, we consider the geometric transform:

$$\begin{cases} r' = r \\ \theta' = \alpha.r + \beta \end{cases} \quad \text{with} \quad \alpha = \frac{\theta_o}{R_1(\theta) - R_2(\theta)} \quad ; \quad \beta = \theta + \frac{R_2(\theta).\theta_o}{R_2(\theta) - R_1(\theta)} \quad (16)$$

where $\theta_0 = \pi/4$ denotes the tilt. We obtain the following Jacobian and transformation matrices:

$$\mathbf{J_{rr'}} = \begin{pmatrix} 1 & 0 \\ -\alpha & c_{22} \end{pmatrix} \quad \Longrightarrow \quad \mathbf{T^{-1}} = \mathbf{R}(\theta) \begin{pmatrix} c_{22} & \alpha r \\ \alpha.r & \dfrac{1 + \alpha^2 r^2}{c_{22}} \end{pmatrix} \mathbf{R}(\theta)^{\mathbf{T}} \quad (17)$$

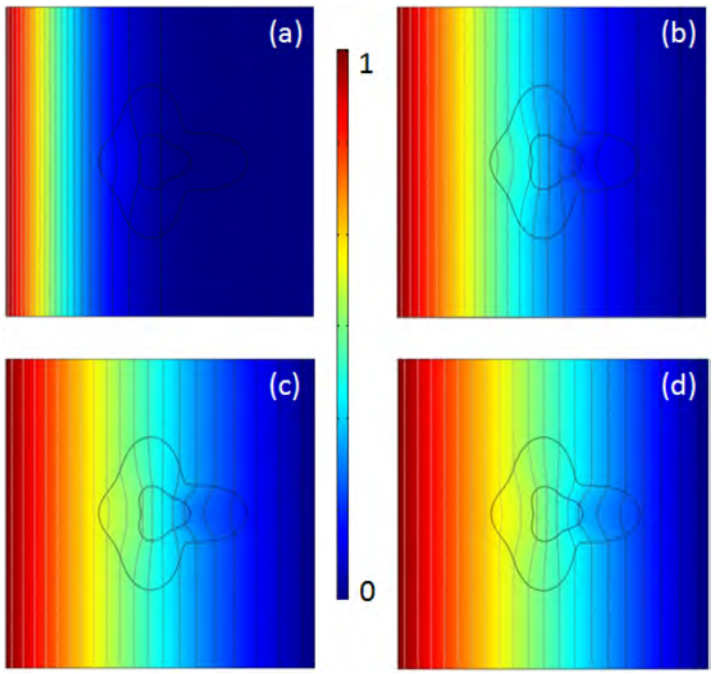

FIG. 4. Diffusion concentrator: Diffusion of heat (or mass) from the left on a concentrator of complex shape of inner radius $R_1(\theta) = 0.4R(1 + 0.2\sin(3\theta))$ and outer radius $R_3(\theta) = R(1 + 0.2(\sin(3\theta) + \cos(4\theta)))$, with $R = 0.4\ 10^{-4}$ m. Snapshots of heat (resp. mass) distribution at $t = 0.001s$ (a), $t = 0.004s$ (b), $t = 0.007$ s (c) and $t = 0.01s$ (d) show that isovalues of temperature (resp. mass) are nearly unperturbed outside the concentrator.

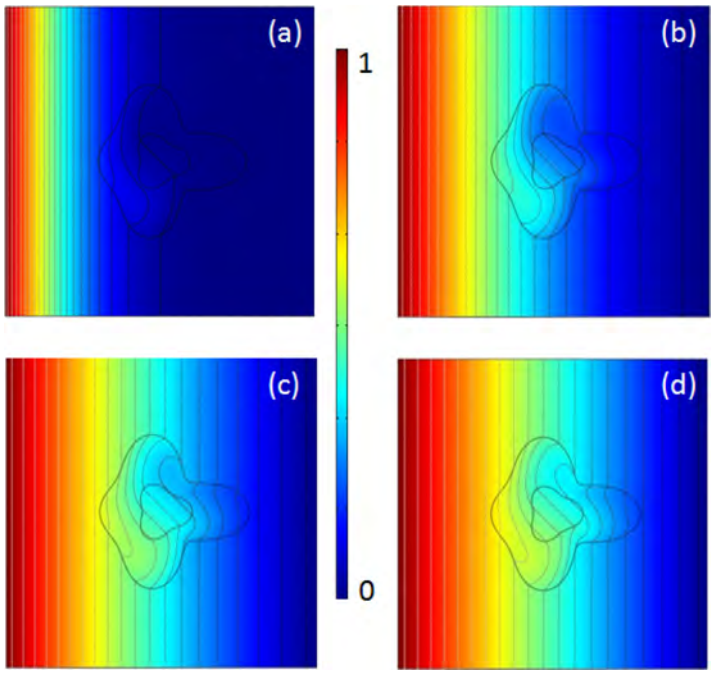

FIG. 5. Diffusion rotator: Diffusion of heat (or mass) from the left on a concentrator of complex shape of inner radius $R_1(\theta) = 0.4R(1 + 0.2\sin(3\theta))$ and outer radius $R_3(\theta) = R(1 + 0.2(\sin(3\theta) + \cos(4\theta)))$, with $R = 0.4\ 10^{-4}$ m and tilt parameter $\theta_0 = \pi/4$. Snapshots of heat (resp. mass) distribution at $t = 0.001s$ (a), $t = 0.004s$ (b), $t = 0.007$ s (c) and $t = 0.01s$ (d) show that isovalues of temperature (resp. mass) are squeezed inside the core and nearly unperturbed outside the rotator.

with $\det(\mathbf{J}) = \frac{r-\beta}{\alpha^2 r}$. Also, we have

$$\begin{aligned} c_{22} &= \frac{\partial\theta}{\partial\theta'} = 1 - \frac{\theta_o.r}{(R_2(\theta)-R_1(\theta))^2}.\left(\frac{\partial R_2(\theta)}{\partial\theta'} - \frac{\partial R_1(\theta)}{\partial\theta'}\right) \\ &\quad - \frac{\theta_o}{(R_2(\theta)-R_1(\theta))^2}\left(R_2(\theta)\frac{\partial R_1(\theta)}{\partial\theta'} - R_1(\theta)\frac{\partial R_2(\theta)}{\partial\theta'}\right) . \end{aligned} \tag{18}$$

D. Three-dimensional diffusion cloak of a complex shape

A nontrivial question to ask is whether one can design thermal or mass diffusion cloaks of non-spherical shapes. The extension of the previous section to the general three-dimensional case requires to describe the inner and outer boundaries of the cloak with varying radii

$$\rho(\theta,\phi) = a_{0,0} + \{\sum_{(m,n)\in N^2\setminus\{(0,0)\}} a_{m,n}\cos(m\theta+n\phi) + b_{m,n}\sin(m\theta+n\phi)\} \tag{19}$$

We further assume there is some revolution for the design with an arbitrary cross-section described by two functions $R_1(\phi)$ and $R_2(\phi)$ giving an angle dependent distance from the origin. These functions correspond respectively to the interior and exterior boundary of the cloak. We shall only assume that these two boundaries can be represented by a differentiable function. Their finite Fourier expansions are thought in the form $R_j(\phi) = a^j_{0,0} + \sum_{n=1}^{p} a^j_{0,n}\cos(n\phi)$, $j = 1,2$, where p can be a small integer, and $a^j_{0,n} = 0$ for $n \neq p$ for computational easiness.

The geometric transformation which maps the field within the full domain $\rho \leq R_2(\phi)$ onto the annular domain $R_1(\phi) \leq \rho' \leq R_2(\phi)$ can be expressed as:[30]

$$\begin{aligned} \rho'(\rho,\phi) &= R_1(\phi) + \rho\frac{R_2(\phi)-R_1(\phi)}{R_2(\phi)} , \\ \theta' &= \theta \ , \ 0 < \theta \leq 2\pi \ , \\ \phi' &= \phi \ , \ -\pi/2 < \phi \leq \pi \end{aligned} \tag{20}$$

where $0 \leq \rho \leq R_2(\phi)$. Note that the transformation maps the field for $\rho > R_2(\phi)$ onto itself through the identity transformation.

This change of coordinates is characterized by the transformation of the differentials through the Jacobian:

$$\mathbf{J}(\rho',\phi') = \frac{\partial(\rho(\rho',\phi'),\theta,\phi)}{\partial(\rho',\theta',\phi')} . \tag{21}$$

After some elementary algebra, we find that

$$\mathbf{T}^{-1} = \begin{pmatrix} \frac{c_{13}^2+\rho^2}{c_{11}\rho'^2} & 0 & -\frac{c_{13}}{\rho'} \\ 0 & c_{11} & 0 \\ -\frac{c_{13}}{\rho'} & 0 & c_{11} \end{pmatrix} \tag{22}$$

with $\det(\mathbf{J}) = \frac{r-\beta}{\alpha^2 r}$.
Also, we have
$c_{11}(\phi') = R_2(\phi')/R_2(\phi') - R_1(\phi')$ and

$$c_{13} = R_2(\phi')\frac{\rho'-R_2(\phi')}{(R_2(\phi')-R_1(\phi'))^2}\frac{dR_1(\phi')}{d\phi'} + R_1(\phi')\frac{R_1(\phi')-\rho'}{(R_2(\phi')-R_1(\phi'))^2}\frac{dR_2(\phi')}{d\phi'} \tag{23}$$

for $R_1(\phi') \leq \rho' \leq R_2(\phi')$. Elsewhere, $\mathbf{T}^{-1}$ reduces to the identity matrix ($c_{11} = 1$ and $c_{13} = 0$ for $\rho' > R_2(\phi')$).

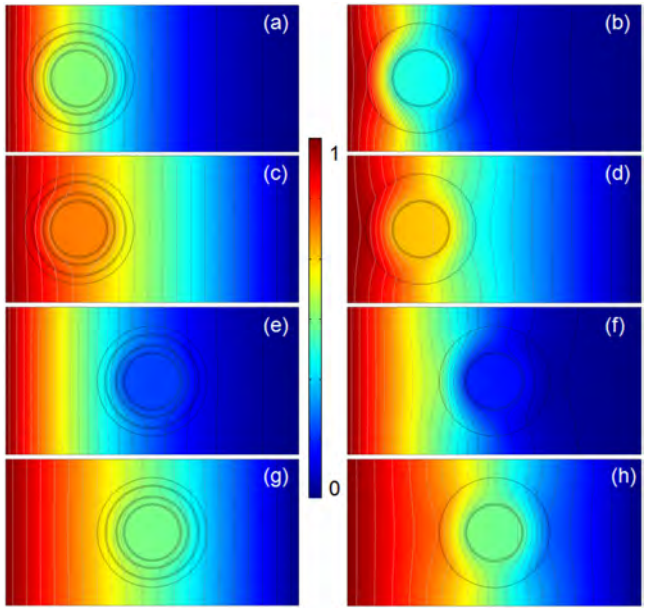

FIG. 6. Layered diffusion cloaks: (Left panel) Diffusion of heat (or mass) from the left on a six-layer cloak of inner radius $R_1 = 1.5\,10^{-4}$ m and outer radius $R_2 = 3\,10^{-4}$ m, consisting of 6 homogeneous layers alternating with interfaces at radii 1.575, 1.9125, 1.9875, 2.5125, and 2.5875 (in unit of $10^{-4}m$) and of respective diffusivities $80, 0.2, 40, 0.4, 10, 0.8$ in a bulk material of diffusivity 1 (in unit of $10^{-5}m^2.s^{-1}$). (Right panel) Diffusion of heat (or mass) from the left on a two-layer cloak of inner radius $R_1 = 1.5\,10^{-4}$ m and outer radius $R_2 = 3\,10^{-4}$ m, consisting of 2 homogeneous with interfaces at radii 1.575 and 2.5875 (in unit of $10^{-4}m$) and of respective diffusivities $80, 0.8$ in a bulk material of diffusivity 1 (in unit of $10^{-5}m^2.s^{-1}$). Panels (a),(b) (resp. (c),(d)) are for a cloak in close proximity to the heat source at $t = 0.004$ s (resp. $t = 0.01$ s); Panels (e), (f) (resp. (g),(h)) are for a cloak farther from the heat source at $t = 0.004$ s (resp. $t = 0.01$ s).

IV. A MULTILAYERED CLOAK WITH SIMPLIFIED ISOTROPIC PARAMETERS

It is interesting to simply the design of diffusion cloaks by considering layered cloaks with homogeneous isotropic layers. As detailed in the introduction, a few papers have already proposed such a route based upon well-known formulae derived notably in the homogenization literature.[29]

A. Two-dimensional layered diffusion cloak

Figure 6 shows snapshots of heat (or concentration in the context of mass diffusion) distribution for a six-layer cloak and a two-layer cloak. At $t = 0.02s$ (a,b,e,f) and $t = 0.12s$ (c,d,g,h) isovalues of temperature (or concentration in the context of mass diffusion) are nearly unperturbed for the six-layer cloak, but not quite so for the two-layer cloak. However, normalized temperature (or concentration) is nonvanishing inside the inner disc of both types of cloaks (and slightly higher for the six-layer one) and depends upon the distance between the center of cloak to the source. The left-hand side has a constant temperature (or concentration) of 1 and the right hand side of 0.

B. Three-dimensional layered diffusion cloak

We now propose a design of a layered spherical cloak for diffusion of heat (resp. mass) based on the homogenization approach. We show in Figure 7 snapshots of heat (resp. mass concentration) for a twenty-layer diffusion cloak. Heat (resp. mass concentration) is clearly shown to be constant inside the invisibility region at every time-step.

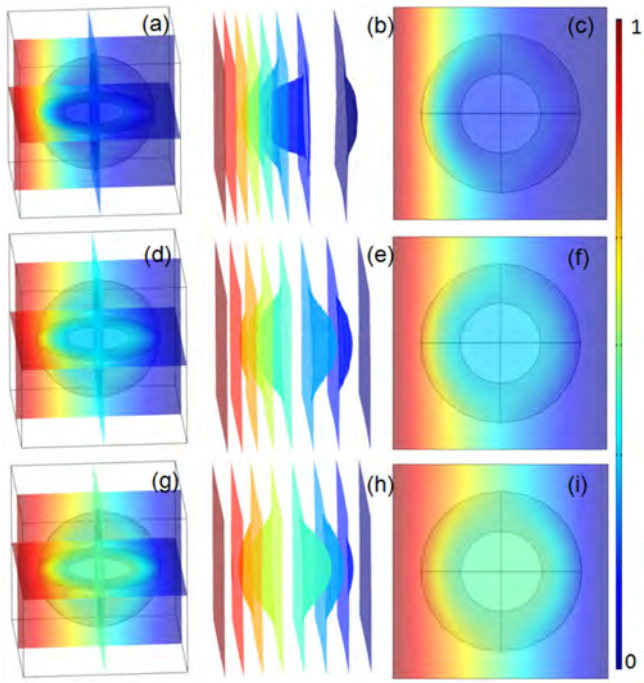

FIG. 7. Layered spherical cloak: Diffusion of heat (or mass) from the left on a cloak of inner radius $R_1 = 1.5\,10^{-6}$ m and outer radius $R_3 = 3.0\,10^{-6}$ m consisting of 20 homogeneous layers of equal thickness and of respective diffusivities (in unit of $10^{-5}.m^2.s^{-1}$), which are $1700, 0.25, 81, 0.25, 30, 0.25, 16.5, 0.25, 11, 0.25, 8, 0.25, 6.5, 0.25, 5.5, 0.25, 4.5, 0.25, 4, 0.25$ (from inner to outer layer). Snapshots of heat distribution at $t = 0.01$ s (a,b,c), $t = 0.015$ s (d,e,f), $t = 0.02$ s (g,h,i) show that isovalues of heat (resp. mass) are nearly unperturbed outside the cloak and the core has uniform heat (resp. mass concentration).

V. DIFFUSION INVISIBILITY CARPET: MAPPING A CURVED SURFACE ON A FLAT SURFACE

Another interesting application of transformational thermodynamics is the concept of carpet cloaks, which is inspired by Li and Pendry's original proposal of invisibility carpets in electromagnetics.[31] For this, let us consider the linear geometric transform:

$$\begin{cases} x' &= x\ ,\ a < x < b\ , \\ y' &= \dfrac{y_2(x) - y_1(x)}{y_2(x)}\, y + y_1(x)\ ,\ 0 < y < y_2(x)\ , \\ z' &= z\ ,\ -\infty < z < +\infty\ , \end{cases} \tag{24}$$

where y' is a stretched vertical coordinate. It is easily seen that this linear geometric transform maps the segment $[a, b]$ within the horizontal axis $y = 0$ onto the curve $y' = y_1(x)$, and leaves the curve $y = y_2(x)$ unchanged. Importantly, there is a one-to-one relationship between the segment and y_1. The curves y_1 and y_2 are assumed to be differentiable, and this ensures that the carpet won't display any singularity on its inner boundary.

A. Two-dimensional carpets

The linear transform (24) is expressed in a Cartesian basis as: $\mathbf{J}_{xx'} = \begin{pmatrix} 1 & 0 \\ \frac{\partial y}{\partial x'} & \frac{1}{\alpha} \end{pmatrix}$ where $\alpha = (y_2 - y_1)/y_1$ and from the chain rule

$$\frac{\partial y}{\partial x'} = y_2 \frac{y' - y_2}{(y_2 - y_1)^2} \frac{\partial y_1}{\partial x} - y_1 \frac{y' - y_1}{(y_2 - y_1)^2} \frac{\partial y_2}{\partial x}\ . \tag{25}$$

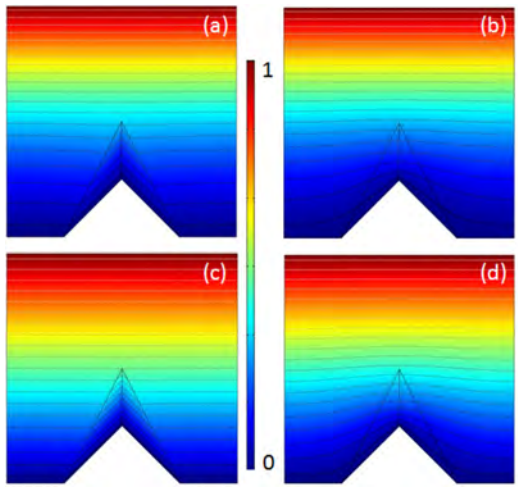

FIG. 8. Thermal (resp. mass diffusion) carpet cloak: (a) carpet (20ms); (b) no carpet (20ms); (c) carpet (50ms); (d) no carpet (50ms). One notes that Dirichlet boundary conditions are set on upper and lower boundaries, with normalised temperature (resp. mass) $u = 1$ on top and $u = 0$ on bottom.

This leads to the inverse symmetric tensor $\mathbf{T}^{-1}$

$$(T^{-1})_{11} = \frac{1}{\alpha}\ ,\ (T^{-1})_{12} = (T^{-1})_{21} = -\frac{\partial y}{\partial x'}\ ,\ (T^{-1})_{22} = \left(1 + \left(\frac{\partial y}{\partial x'}\right)^2\right)\alpha\ . \tag{26}$$

We note that the transformed product of density and specific heat has the factor $\det(\mathbf{J}) = \alpha^{-1} = y_1/(y_2 - y_1)$ which is spatially varying, but non-vanishing. When the carpet's boundaries are piecewise linear, which is the case in Fig. 8, one gets piecewise constant, anisotropic, coefficients. Figure 8 clearly demonstrates the functionality of an invisibility carpet for heat (or mass) diffusion: isothermal lines curved by the presence of a cold boundary, see Figs. 8(b) and 8(d) are straightened by the carpet, see Figs. 8(a) and 8(c). It should be noted that the temperature (resp. mass concentration) needs to be uniform all throughout the lower boundary of the computational domain for the carpet to work properly. Moreover, when the protruding object is narrower, the required anisotropy in the carpet is larger.

B. Three-dimensional carpets

It is also possible to hide protrusions on a surface. For this, let us consider the linear geometric transform parameterized by $t \in (0, 2\pi)$:

$$\begin{cases} x'(t) &= x(t)\ ,\ a(t) < x(t) < b(t)\ , \\ y'(t) &= y(t)\ ,\ c(t) < y(t) < d(t)\ , \\ z'(t) &= \dfrac{z_2(x(t), y(t)) - z_1(x(t), y(t))}{z_2(x(t), y(t))} z(t) + z_1(x(t), y(t))\ ,\ 0 < z(t) < f_2(x(t), y(t))\ , \end{cases} \tag{27}$$

where y' is a stretched vertical coordinate. It is easily seen that this linear geometric transform maps the arbitrary domain $D = \bigcup_{t\in(0,2\pi)}\{[a(t), b(t)] \times [c(t), d(t)]\}$ within the plane xy onto the surface $z' = z_1(x, y)$, and leaves the surface $z = z_2(x, y)$ unchanged. Importantly, there is a one-to-one correspondence between the domain D and the surface $z' = z_1$. The surfaces z_1 and z_2 are assumed to be differentiable, and this ensures that the carpet won't display any singularity on its inner boundary.

The linear transform (27) is expressed in a Cartesian basis as: $\mathbf{J}_{xx'} = \begin{pmatrix} 1 & 0 & 0 \\ 0 & 1 & 0 \\ \frac{\partial z}{\partial x'} & \frac{\partial z}{\partial y'} & \frac{1}{\alpha} \end{pmatrix}$ where $\alpha = [z_2(x(t), y(t)) - z_1(x(t), y(t)]/z_2(x(t), y(t))$ and from the chain rule

$$\begin{aligned} \frac{\partial z}{\partial x'} &= z_2 \frac{z' - z_2}{(z_2 - z_1)^2} \frac{\partial z_1}{\partial x} - z_1 \frac{z' - z_1}{(z_2 - z_1)^2} \frac{\partial z_2}{\partial x}, \\ \frac{\partial z}{\partial y'} &= z_2 \frac{z' - z_2}{(z_2 - z_1)^2} \frac{\partial z_1}{\partial y} - z_1 \frac{z' - z_1}{(z_2 - z_1)^2} \frac{\partial z_2}{\partial y}. \end{aligned} \tag{28}$$

This leads to the inverse symmetric tensor $\mathbf{T}^{-1}$ which is fully described by seven nonvanishing entries in a Cartesian basis:

$$\begin{aligned} (T^{-1})_{11} &= (T^{-1})_{22} \frac{1}{\alpha} \quad , (T^{(-1)})_{13} = (T^{-1})_{31} = -\frac{\partial z}{\partial x'} \\ (T^{-1})_{23} &= (T^{-1})_{32} = -\frac{\partial z}{\partial y'} \quad , (T^{-1})_{33} = \left(1 + \left(\frac{\partial z}{\partial x'}\right)^2 + \left(\frac{\partial z}{\partial y'}\right)^2\right) \alpha \end{aligned}$$

We note that the transformed product of density and specific heat has the factor $\det(\mathbf{J}) = \alpha^{-1} = z_1/(z_2 - z_1)$ which is spatially varying, but non-vanishing. In a way similar to two-dimensional carpets, it can be seen that 3D carpets with flat boundaries consist of regions with piecewise homogeneous anisotropic diffusivity.

VI. CONCLUDING REMARKS

In this review article, we have shown that one can control diffusion processes in the context of heat or mass thanks to geometric transformations in the convection-diffusion equations. The required heterogeneous anisotropic diffusivity inside the cloaks can be replaced by concentric layers with isotropic homogeneous diffusivity which achieve a remarkably enhanced control of diffusion, in the case of circular, or spherical, geometries. In the case of cloaks, concentrators and rotators of an arbitrary shape, the path toward an approximate design remains a challenge. We have also discussed the possibility of designing invisibility carpets for diffusion processes. In this latter case, one need only achieve a minimum level of control on isothermal values in order to reduce backscattered diffusion, which makes the metamaterial parameters easier to achieve: there is no singularity in the required tensor of diffusivity due to the fact that we use a one-to-one mapping.

ACKNOWLEDGMENTS

This work has been carried out thanks to the support of the A*MIDEX project (no ANR-11-IDEX-0001-02) funded by the Investissements d'Avenir French Government program, managed by the French National Research Agency (ANR). S.G. is also thankful for an ERC grant ANAMORPHISM. D.P. acknowledges funding from CNRS/DGA and C.A., M.Z., S.G. acknowledge further funding from ANR (project INPACT).

[1] C. Z. Fan, Y. Gao, and J. P. Huang, "Shaped graded materials with an apparent negative thermal conductivity," Appl. Phys. Lett. **92**, 251907 (2008).
[2] J. Y. Li, Y. Gao, and J. P. Huang, "A bifunctional cloak using transformation media," J. Appl. Phys. **108**, 074504 (2010).
[3] S. Narayana and Y. Sato, "Heat flux manipulation with engineered thermal materials," Phys. Rev. Lett. **108**, 214303 (2012).
[4] F. Gomory, M. Solovyov, J. Souc, C. Nacau, J. Prat-Camps, and A. Sanchez, "Experimental realization of a magnetic cloak," Science **335**, 1466 (2012).
[5] T. Han, T. Yuan, B. Li, and C.-W. Qiu, "Homogeneous thermal cloaks with constant conductivity and tunable heat localization," Sci. Rep. **3**, 1593 (2013).
[6] E. M. Dede, T. Nomura, P. Schmalenberg, and J. S. Lee, "Heat flux cloaking, focusing, and reversal in ultra-thin composites considering conduction-convection effects," Appl.Phys. Lett. **103**, 063501 (2013).
[7] H. Xu, X. Shi, F. Gao, H. Sun, and B. Zhang, "Ultrathin three-dimensional thermal cloak," Phys. Rev. Lett. **112**, 054301 (2014).
[8] S. Guenneau, C. Amra, and D. Veynante, "Transformation thermodynamics : cloaking and concentrating heat flux," Opt. Express **20**(7), 8207–8218 (2012).

[9] R. Schittny, M. Kadic, S. Guenneau, and M. Wegener, "Experiments on transformation thermodynamics: Molding the flow of heat," Phys. Rev. Lett. **110**(19), 195901 (2013).
[10] H. Xu, X. Shi, F. Gao, H. Sun, and B. Zhang, "Experimental demonstration of an ultra-thin three-dimensional thermal cloak," Phys. Rev. Lett. **112**, 054301 (2014).
[11] T. Han, X. Bai, D. Gao, J. T. L. Thong, B. Li, and C.-W. Qiu, "Experimental demonstration of a bilayer thermal cloak," Phys. Rev. Lett. **112**, 054302 (2014).
[12] T. Han, X. Bai, J. T. Thong, B. Li, and C.-W. Qiu, "Full control and manipulation of heat signatures: Cloaking, camouflage and thermal metamaterials," Adv. Mater. **26**, 1731–1734 (2014).
[13] D. Petiteau, S. Guenneau, M. Bellieud, M. Zerrad, and C. Amra, "Spectral effectiveness of engineered thermal cloaks in the frequency regime," Sci. Rep. **4**, 7386 (2014).
[14] M. Rahm, D. Schurig, D. A. Roberts, S. A. Cummer, D. R. Smith, and J. B. Pendry, "Design of electromagnetic cloaks and concentrators using form-invariant coordinate transformations of Maxwell's equations," Photon. Nanostruct. Fundam. Appl. **6**, 87–95 (2008).
[15] S. Guenneau and C. Amra, "Anisotropic conductivity rotates heat fluxes in transient regimes," Opt. Express **21**(5), 6578–6583 (2013).
[16] S. Guenneau and T. M. Puvirajesinghe, "Fick's second law transformed : one path to cloaking in mass diffusion," J. Roy. Soc. Interface **10**, 20130106 (2013).
[17] Z. Lunwu and S. Runxia, "Controlling chloride ions diffusion in concrete," Sci. Rep. **3**, 3359 (2013).
[18] R. Schittny, M. Kadic, T. Buckmann, and M. Wegener, "Invisibility cloaking in a diffusive light scattering medium," Science **345**(6195), 427–429 (2014).
[19] U. Leonhardt, "Applied Physics: Cloaking of heat," Nature **498**, 440–441 (2013).
[20] A. Alu, "Thermal cloaks get hot," Physics **7**, 12 (2014).
[21] J. B. Pendry, D. Schurig, and D. R. Smith, "Controlling electromagnetic fields," Science **312**, 1780–1782 (2006).
[22] U. Leonhardt, "Optical conformal mapping," Science **312**, 1777–1780 (2006).
[23] G. W. Milton, M. Briane, and J. R. Willis, "On cloaking for elasticity and physical equations with a transformation invariant form," New J. Physics **8** (2006).
[24] A. Greenleaf, Y. Kurylev, M. Lassas, and G. Uhlmann, "Full-wave invisibility of active devices at all frequencies," Comm. Math. Phys. **275**(3), 749–789 (2007).
[25] S. A. Cummer and D. Schurig, "One path to acoustic cloaking," New J. Phys. **9**, 45 (2007).
[26] H. Chen and C. T. Chan, "Acoustic cloaking in three dimensions using acoustic metamaterials," Appl. Phys. Lett. **91**, 183518 (2007).
[27] M. Brun, S. Guenneau, and A. B. Movchan, "Achieving control of in-plane elastic waves," Appl. Phys. Lett. **94**, 061903 (2009).
[28] M. Maldovan, "Sound and heat revolutions in phononics," Nature **503**, 209–217 (2013).
[29] V. V. Jikov, S. M. Kozlov, and O. A. Oleinik, *Homogenization of Differential Operators and Integral Functionals* (Springer-Verlag, New-York, 1994).
[30] A. Nicolet, F. Zolla, Y. O. Agha, and S. Guenneau, "Geometrical transformations and equivalent materials in computational electromagnetism," International Journal for Computation and Mathematics in Electrical and Electronic Engineering, COMPEL **27**, 806–819 (2008).
[31] J. Li and J. B. Pendry, "Hiding under the Carpet: A new strategy for cloaking," Phys. Rev. Lett. **101**, 203901 (2008).